

The Effect of Photocrosslinkable Groups on Thermal Stability of Bulk Heterojunction Solar Cells Based on Donor–Acceptor-Conjugated Polymers

Xun Chen,¹ Lie Chen,^{1,2} Yiwang Chen^{1,2}

¹Institute of Polymers/Department of Chemistry, Nanchang University, 999 Xuefu Avenue, Nanchang 330031, China

²Jiangxi Provincial Key Laboratory of New Energy Chemistry, Nanchang University, 999 Xuefu Avenue, Nanchang 330031, China

Correspondence to: L. Chen (E-mail: chenlienc@163.com)

Received 16 March 2013; accepted 7 June 2013; published online 3 July 2013

DOI: 10.1002/pola.26828

ABSTRACT: Three different types of photocrosslinkable groups into a low band-gap donor–acceptor-conjugated polymer, namely poly{benzo[1,2-*b*:4,5-*b'*]dithiophene-*alt*-thieno[3,4-*b*]thiophene} (PBT), were developed to comparatively investigate the effect of the photocrosslinkable groups on the thermal stability of bulk heterojunction solar cells. Compared with vinyl groups, bromine- and azide- photocrosslinkable groups are more prompt for photocrosslinking to yield a denser crosslinking network, probably due to the different crosslinking mechanisms and reaction rates. In contrast to the reference device decreasing to less than 10% of its initial efficiency value after 80 h of annealing at 150 °C, a great improvement in the thermal stability of performance of all these crosslinked functional copolymers devices demonstrates that photocrosslinking can effectively improve the thermal stability of the

active layer by suppressing [6,6]-phenyl-C₆₁-butyric acid methyl diffusion and phase separation. Furthermore, the solar cells with crosslinked bromine- and azide-functionalized PBT polymers showed very thermally stable photovoltaic device performance by retaining 78 and 66% of their initial device efficiency, respectively, whereas vinyl-functionalized PBT devices retained only 51% of its initial value after long-time thermal annealing. This suggests that an appropriate crosslinking network with homogenous active morphology could dramatically enhance the device stability without sacrificing the performance. © 2013 Wiley Periodicals, Inc. *J. Polym. Sci., Part A: Polym. Chem.* **2013**, *51*, 4156–4166

KEYWORDS: conjugated polymers; crosslinking; photoreaction; thermal stability

INTRODUCTION Polymer bulk heterojunction (BHJ) solar cells have drawn much attention in the past decade due to their low-cost, mechanical flexibility, easy fabrication, and the general applicability of organic materials.^{1–3} Recently, the power conversion efficiency (PCE) in excess of 8% has been demonstrated by several groups and constitutes a significant breakthrough in the field of organic solar cells.^{4,5} A key parameter for efficient BHJ solar cells is the three-dimensional bicontinuous and nanometer-scale morphology of the active layer that provides a large interfacial area for exciton dissociation. In optimized BHJ, phase separation of the electron donor and the electron acceptor domains should be on the same length-scale as the exciton diffusion length, facilitating efficient exciton harvesting and then resulting in improved device performance. The optimal morphology in such polymer/fullerene BHJ solar cells can be controlled by process optimization involving the vapor pressure of the solvent,⁶ the rate of solvent removal,⁷ the addition of chemical additives,^{8,9} thermal annealing treatments, and solvent annealing.^{10,11} Although all of these strategies are efficient to improve the morphology of the BHJ

blend, the high-performance morphology only represents a metastable state, which cannot usually be maintained over long operation times. In fact, most BHJ systems show poor stability and often undergo macrophase segregation of the blend components, especially after prolonged exposure to heat.¹² It has been reported that a prolonged thermal annealing induces the formation of large aggregates of fullerene derivative, which deteriorates the device performance.¹³ Considering that normal BHJ photovoltaic device operation may subject the active layer to large temperature fluctuations, improving the robustness of the BHJ with respect to thermal stability is critical.¹⁴

Several studies have been reported on improving the thermal stability of conjugated polymer-fullerene BHJ photovoltaic devices.^{15–17} One consists of the use of compatibilizers having two different blocks of conjugated polymers and fullerenes to act as a compatibilizer reducing the interfacial tension between the two dissimilar components of the BHJ thus retarding their phase separation.¹⁸ However, this approach has not been so successful, presumably since the

synthesis of a compatibilizer often requires multiple postpolymerization steps and suffers from the low solubility of fullerenes. Another strategy explored the use of thermally crosslinkable units such as an epoxide-functionalized fullerene derivative as a means to prevent phase segregation on one of the materials. Unfortunately, the crosslinking led to significantly reduced device performance in spite of the stabilized active layer morphology.^{19,20} Yet another approach that is also explored in this work is to incorporate crosslinkable groups into conjugated polymers side chains.^{21,22} This crosslinking strategy is a simple and powerful solution for achieving long-term thermal stability of BHJ solar cells. Recent studies reported that such crosslinking is generally mediated by a bimolecular reaction between specific functional groups, with the crosslinking reactions being activated by either heat (thermal)^{23,24} or ultraviolet (UV) light.^{25,26} However, in contrast to thermal crosslinking, photocrosslinking does not interfere with the thermal treatments that are often needed during device optimization; thus, this process allows for morphology optimization with independent control of crosslinking and thermal annealing. A library of photocrosslinkable copolymers containing some light-sensitive substituents such as alkyl-bromide,^{21,22} azide,²⁷⁻²⁹ and vinyl^{30,31} for use as p-type materials has been reported on the thermal stability of the BHJ morphology. Utilizing these materials, it was shown that even after long time of annealing at an elevated temperature of 150 °C, the devices containing the photocrosslinkable copolymer within the active layer were able to retain their initial PCE. This result was attributed to the stabilizing effect of the photocrosslinked copolymer on the nanoscale morphology of the active layer.

Although several different photocurable groups have been used for stabilizing the active layer morphology by photochemical crosslinking methods, previous studies have only focused on one specific crosslinking reaction. To gain a deeper insight on effect of photocrosslinking on the morphology of active layer and how the crosslinkable groups influence the device stability, herein, we developed a comparative study between three different types of photocrosslinkable functionalities for stabilizing the BHJ film morphology. With relatively simple means bromine, azide, and vinyl photocrosslinking groups have been incorporated into the side chains of the low band-gap copolymer poly{benzo[1,2-*b*:4,5-*b'*]dithiophene-alt-thieno[3,4-*b*]-thiophene} (PBT). The effects of these different photocrosslinkable functional copolymers on BHJ morphology under long-term exposure to heat were investigated by atomic force microscopy (AFM) and transmission electron microscopy (TEM). We also studied the long-term performances of BHJ solar cells made of these functional copolymers as electron donors in combination with [6,6]-phenyl-C₆₁-butyric acid methyl ester (PCBM) as acceptor and compare them to the pristine PBT/PCBM system.

EXPERIMENTAL

Materials

1-Octanol, 8-bromo-1-octanol, 7-octen-1-ol, 4-(dimethylamino)pyridine and *N,N'*-dicyclohexylcarbodiimide (DCC) were pur-

chased from Alfa Aesar and without any further purification. Other chemicals were obtained from Shanghai Reagent and used as received. Dichloromethane (CH₂Cl₂) and toluene were dried and freshly distilled under nitrogen before use. Indium tin oxide (ITO) glass was purchased from Delta Technologies, whereas PEDOT:PSS (Baytron PA14083) was obtained from Bayer.

Techniques

The nuclear magnetic resonance (NMR) spectra were collected on a Bruker ARX 400 NMR spectrometer with deuterated chloroform as the solvent and with tetramethylsilane ($\delta = 0$) as the internal standard. The gel permeation chromatography (GPC) was conducted with a Breeze Waters system equipped with a Rheodyne injector, a 1515 Isocratic pump, and a Waters 2414 differential refractometer using polystyrenes as the standard and tetrahydrofuran (THF) as the eluent at a flow rate of 1.0 mL min⁻¹ and 40 °C through a Styragel column set, Styragel HT3 and HT4 (19 × 300 mm², 10³ + 10⁴ Å) to separate molecular weight (MW) ranging from 10² to 10⁶. Thermogravimetric analysis (TGA) was performed on a PerkinElmer TGA 7 for thermogravimetry at a heating rate of 10 °C min⁻¹ under nitrogen with a sample size of 8–10 mg. The cyclic voltammetry (CV) was performed on a CHI660C potentiostat equipped with electrochemical analysis system software and standard three-electrode configuration under an argon atmosphere at RT and a scan rate of 50 mV s⁻¹. Platinum rod, platinum wire, and saturated calomel electrode were used as working electrode, counter electrode, and reference electrode in a 0.1 mol L⁻¹ 1 Bu₄NPF₆-acetonitrile solution, respectively. The ultraviolet-visible (UV) spectra of the samples were recorded on a PerkinElmer Lambda 750 spectrophotometer. The infrared (IR) spectra were recorded on a Shimadzu IR Prestige-21 Fourier transform IR (FTIR) spectrophotometer by drop-casting sample solution on KBr substrates. Texture observations by polarizing optical microscopy (POM) were made with a Nikon E600POL POM equipped with an Instec HS 400 heating and cooling stage. The X-ray diffraction (XRD) study of the samples was carried out on a Bruker D8 Focus XRD operating at 30 kV and 20 mA with a copper target ($\lambda = 1.54$ Å) and at a scanning rate of 1 °/min. AFM measurement was carried out using a Digital Instrumental Nanoscope 31 operated in the tapping mode. TEM images were recorded using a JEOL-2100F transmission electron microscope and an internal charge-coupled device camera.

Device Fabrication and Characterization

The structure of the devices was ITO/PEDOT:PSS/polymer:PCBM/LiF/metal cathode. Before use, the glass substrates were ultrasonicated for 20 min in acetone followed by deionized water and then 2-propanol. The substrates were dried under a stream of nitrogen and subjected to the treatment of UV ozone over 30 min. A filtered dispersion of PEDOT:PSS in water (Baytron Al4083) was then spun-cast onto clean ITO substrates at 4000 rpm for 60 s and then baked at 140 °C for 10 min. The polymer:PCBM (1:1 wt) blend solution (10 mg mL⁻¹ in 1,2-dichlorobenzene) was spin-coated on the PEDOT:PSS layers at 1000 rpm for 30 s, and the thickness of film was ~ 80 nm. UV-mediated photocrosslinking was then

performed on the blend cast films, by irradiating them with a low-power UV lamp at 254 nm (21 mW cm^{-2}). Finally, electrodes were deposited on top of the active layer via thermal evaporation. A 0.8-nm layer of LiF followed by a 100-nm layer of Al were evaporated under vacuum ($<10^{-6}$ Torr) to form the electrodes. Current-voltage (J - V) characteristics were recorded using Keithley 2400 Source Meter in the dark and by 100 mW cm^{-2} simulated AM 1.5 G irradiation (Abet Solar Simulator Sun2000).

Crosslinking Experiments

Photocrosslinking was carried out in a nitrogen-filled glove box by irradiating the polymer films with UV light ($\lambda = 254 \text{ nm}$) from a low-power hand-held lamp (21 mW cm^{-2}). To evaluate the extent of photocrosslinking, the irradiated polymer films were immersed into chlorobenzene for 5 min, followed by rinsing with acetone for 3 min and then dried under a stream of nitrogen. UV-vis absorption spectra were then recorded on the polymer films after irradiation and solvent washing, and compared to the UV-vis absorption spectra of the same polymer films before irradiation.

Synthesis

General

4,6-dibromo-thieno[3,4-*b*]thiophene-2-carboxylic acid (**1**) was synthesized according to the procedure reported in literature.³²

Synthesis of Octyl 4,6-Dibromothieno[3,4-*b*]thiophene-2-carboxylate (**2a**)

To the mixture of compound **1** (0.68 g, 2.0 mmol), DCC (0.50 g, 2.4 mmol) and 4-(dimethylamino)pyridine (DMAP) (84 mg, 0.69 mmol) in a 50-mL round-bottom flask with 20 mL CH_2Cl_2 were added 1-octanol (1.3 g, 10.0 mmol). The mixture was stirred for 24 h under N_2 atmosphere, was poured into 30-mL water, and then extracted with CH_2Cl_2 . The organic phase was dried with sodium sulfate and the solvent was removed. The product was purified with column chromatography on silica gel using hexane/ CH_2Cl_2 (4:1), yielding the pure compound as a light orange solid 0.63 g (67%).

$^1\text{H NMR}$ (CDCl_3 , 400 MHz): δ (ppm) 7.53 (1H, m, Ar-H), 4.31 (2H, m, $-\text{OCH}_2$), 1.88 (2H, m, $-\text{OCH}_2\text{CH}_2$), 1.52-1.21 (10H, m, $(\text{CH}_2)_5$), 0.95 (3H, t, CH_3).

Synthesis of 8-Bromooctyl 4,6-Dibromothieno[3,4-*b*]thiophene-2-carboxylate (**2b**)

Prepared as for **2a**: compound **1** (0.68 g, 2.0 mmol), DCC (0.50 g, 2.4 mmol), DMAP (84 mg, 0.69 mmol), and 8-bromo-1-octanol (2.09 g, 10.0 mmol) were dissolved in CH_2Cl_2 (20 mL). Yield 0.68 g (62%).

$^1\text{H NMR}$ (CDCl_3 , 400 MHz): δ (ppm) 7.53 (1H, m, Ar-H), 4.31 (2H, m, $-\text{OCH}_2$), 3.41 (2H, t, $-\text{CH}_2\text{Br}$), 1.88 (2H, m, $-\text{OCH}_2\text{CH}_2$), 1.75 (2H, t, $\text{BrCH}_2\text{CH}_2-$), 1.52-1.21 (10H, m, $(\text{CH}_2)_4$).

Synthesis of 7-Octenyl 4,6-Dibromothieno[3,4-*b*]thiophene-2-carboxylate (**2c**)

Prepared as for **2a**: compound **1** (0.68 g, 2.0 mmol), DCC (0.50 g, 2.4 mmol), DMAP (84 mg, 0.69 mmol), and 7-octen-

1-ol (1.28 g, 10.0 mmol) were dissolved in CH_2Cl_2 (20 mL). Yield 0.61 g (65%).

$^1\text{H NMR}$ (CDCl_3 , 400 MHz): δ (ppm) 7.53 (1H, m, Ar-H), 5.87 (1H, m, $-\text{CH}=\text{CH}_2$), 5.03 (2H, m, $-\text{CH}=\text{CH}_2$), 4.31 (2H, m, $-\text{OCH}_2$), 2.07 (2H, m, $-\text{CH}_2\text{CH}=\text{CH}_2$), 1.87 (2H, m, $-\text{OCH}_2\text{CH}_2$), 1.52-1.21 (6H, m, $(\text{CH}_2)_3$).

Synthesis of Polymer PBT

Monomer **2a** (0.21 g, 0.50 mmol) was weighed into a 25-mL round-bottom flask. 2,6-bis(trimethyltin)-4,8-bis-(2-ethyl-hexyloxy)benzo[1,2-*b*:4,5-*b'*]dithiophene (BDT) (0.39 g, 0.50 mmol) and $\text{Pd}(\text{PPh}_3)_4$ (25 mg) were added. The flask was subjected to three successive cycles of vacuum followed by refilling with argon. Then, anhydrous DMF (2 mL) and anhydrous toluene (8 mL) were added via a syringe. The polymerization was carried out at 110°C for 12 h under nitrogen protection. The polymer was precipitated in methanol, isolated by centrifugation, purified by sequential Soxhlet extractions using methanol, hexane, and chloroform, respectively. The chloroform fraction was dried to yield the final polymer (0.34 g, 85% yield).

Synthesis of Polymer PBT-Br

Prepared as for PBT: Monomer **2a** (0.15 g, 0.35 mmol) and monomers **2b** (75 mg, 0.15 mmol) (**2a**: **2b** = 7:3 molar ratio), BDT (0.39 g, 0.50 mmol), and $\text{Pd}(\text{PPh}_3)_4$ (25 mg) were dissolved in DMF/toluene (2 mL/8 mL). Yield 0.32 g (80%).

Synthesis of Polymer PBT-Vinyl

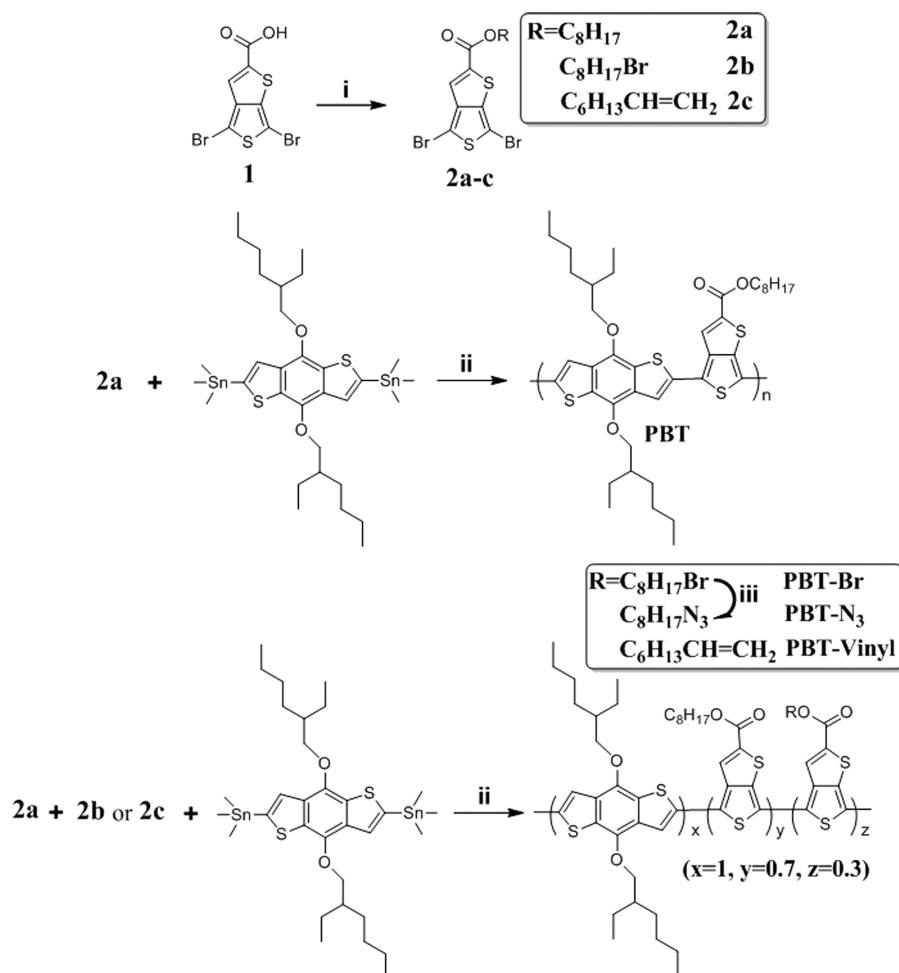
Prepared as for PBT: Monomer **2a** (0.15 g, 0.35 mmol) and monomers **2c** (60 mg, 0.15 mmol) (**2a**: **2c** = 7:3 molar ratio), BDT (0.39 g, 0.50 mmol), and $\text{Pd}(\text{PPh}_3)_4$ (25 mg) were dissolved in DMF/toluene (2 mL/8 mL). Yield 0.30 g (78%).

Synthesis of Polymer PBT- N_3

PBT-Br (0.3 g) was dissolved in toluene (100 mL) at 100°C and sodium azide (0.31 g, 4.83 mmol) in DMF (100 mL) was added slowly. The mixture was stirred at 100°C under argon for 48 h. The solvents were removed under reduced pressure and the polymer redissolved in chloroform and precipitated in methanol. The polymer was purified by Soxhlet extraction first with methanol then with chloroform and finally precipitated in methanol. Yield: 0.29 g (95%).

RESULTS AND DISCUSSION

A low band-gap alternating conjugated polymers based on BDT units as electron donors and thieno[3,4-*b*]thiophene (TT) units as electron acceptors, namely PBT, are an important family of photovoltaic materials. For additional improvements in stabilizing the BHJ morphology, in this work, structural modifications brought about by using different substituents such as alkyl-vinyl, bromine and azide on PBT (note PBT-vinyl, PBT-Br, and PBT- N_3 , respectively) allowing for photocrosslinking of the polymers in device. The monomers and the four polymers were synthesized as shown in



SCHEME 1 Synthesis of the monomers **2a-c** and subsequent polymerization with 2,6-bis(trimethyltin)-4,8-bis-(2-ethyl-hexyloxy)-benzo[1,2-*b*:4,5-*b'*]dithiophene) to give the polymers with different functionalities in the side chains. i: DCC, DMAP, CH_2Cl_2 ; ii: $Pd(PPh_3)_4$, toluene/DMF; and iii: NaN_3 , toluene/DMF.

Scheme 1. The carboxyl groups in 4,6-dibromo-thieno[3,4-*b*]thiophene-2-carboxylic acid (**1**) were substituted by a typical esterification with either 1-octanol or bromine- and vinyl-substituted alkyl alcohol respectively, to yield different photocrosslinkable TT-based monomers (**2a-c**). Polymerization reactions to give the copolymers PBT-Br and PBT-vinyl were performed through a Stille coupling between 2,6-bis(trimethyltin)-4,8-bis-(2-ethyl-hexyloxy)-BDT monomer and a mixture of **2a** and **2b** or **2c**. A monomer feed ratio of **2b** or **2c** to **2a** was chosen to be 3:7 which should provide sufficient crosslinkable groups per polymer chain to give the high photocrosslinking efficiency.^{21,28,33} The synthesis of PBT- N_3 was carried out by treating PBT-Br with NaN_3 in a hot toluene-DMF mixed solution, replacing bromine with an azide units (N_3). Then, residual NaN_3 was removed by Soxhlet purification using methanol. The complete azide units substitution of the PBT-Br copolymer was evidenced by the shift of the 1H NMR resonance of the methylene group ($\delta = 3.45$ ppm) in α to the terminal bromine atom (Fig. 1). Moreover, the polymer PBT was also been prepared for comparison. The molecular weights were estimated by GPC using

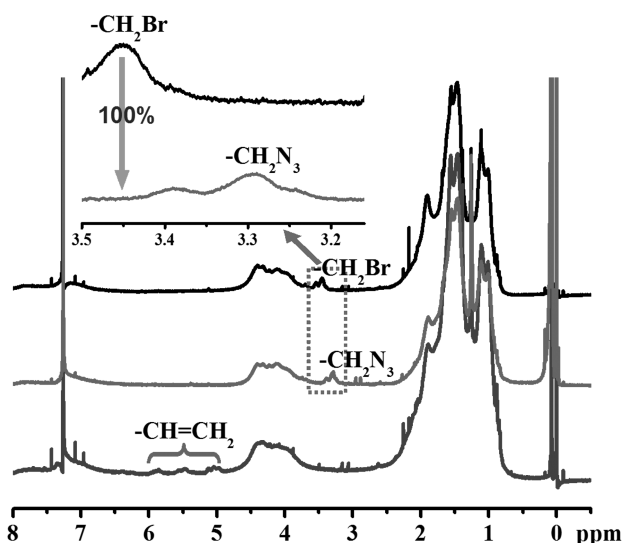


FIGURE 1 1H NMR spectra of the polymers PBT-vinyl, PBT-Br, and PBT- N_3 .

TABLE 1 Physical Properties and Photoelectric Data for the Four Polymers

Polymer	T_d ($^{\circ}\text{C}$)	M_n (kg mol^{-1})	PDI	λ_{max} (nm)	λ_{max}^a (nm)	$E_g^{\text{opt}}/E_g^{\text{CV}}$ (eV)	E_{HOMO} (eV)	E_{LUMO} (eV)
PBT	322	23.5	2.1	654	654	1.6/1.72	-5.18	-3.46
PBT-vinyl	322	20.7	2.3	651	649	1.6/1.68	-5.16	-3.48
PBT-Br	321	21.9	2.2	652	651	1.6/1.77	-5.21	-3.44
PBT- N_3	320	21.3	2.2	652	650	1.6/1.78	-5.19	-3.41

^a Measured in the crosslinked film. $E_{\text{HOMO}} = -(E_{\text{ox}} + 4.40)$ eV and $E_{\text{LUMO}} = -(E_{\text{red}} + 4.40)$ eV. The electrochemical band gap (E_g^{CV}) was calculated on the formula, $E_g^{\text{CV}} = E_{\text{LUMO}} - E_{\text{HOMO}}$.

THF as the eluent (Table 1). Thermal properties of the polymers were determined by TGA under nitrogen atmosphere at a heating rate of $10\text{ }^{\circ}\text{C min}^{-1}$. The four polymers have good thermal stability with 5% weight loss temperatures almost at $321\text{ }^{\circ}\text{C}$ as shown in Figure 2. This indicates that the incorporation of different photocrosslinkable units does not change the thermal stability when compared with the pristine PBT copolymer. Obviously, the thermal stability of these polymers is adequate for their applications in BHJ solar cells and other optoelectronic devices.

Electrochemical CV has been widely employed to investigate the electrochemical behavior of the polymers and estimate its highest occupied molecular orbital (HOMO) and lowest unoccupied molecular orbital (LUMO) energy levels. The HOMO and LUMO energy levels of the polymers were calculated from the onset oxidation potential and the onset reduction potential according to the equations.³⁴ Figure 3 shows the cyclic voltammogram curves of the four polymers. Based on the onset potentials, the HOMO and LUMO energy levels of the pure PBT polymer are estimated to be -5.18 and -3.46 eV, respectively. After functionalized with vinyl, bromine, and azide groups at the side chains, the LUMO and HOMO levels for the three functionalized copolymers PBT-vinyl, PBT-Br, and PBT- N_3 keep almost unchanged, as listed

in Table 1. This indicates that introduction of photocurable groups into the polymer side chain does not significantly affect the electrochemical properties of the polymers.

Polymers bearing vinyl, bromine and azide units can be easily photocrosslinking under UV irradiation via different chemical reaction mechanisms. The bromo-alkyl group is presumably cleaved homolytically to give an alkyl radical and a bromine radical³⁵ while the alkyl azide group splits off molecular nitrogen (N_2) leaving an alkyl nitrene.^{36,37} The photoinduced crosslinking through vinyl groups may be take place by a 2+2 Diels-Alder cycloaddition.³⁸ The efficiencies of the photocrosslinking of these functional polymers were investigated by the insolubility of the films in organic solvents as monitored by UV-vis absorption spectra. Figure 4 shows the photocrosslinking behaviors of these functional PBT polymers as a function of UV exposure time in the range of 0–30 min. The pristine PBT polymer did not crosslink under these conditions. PBT-vinyl, PBT-Br, and PBT- N_3 were spun cast from dichlorobenzene (DCB) solution to produce films of approximately 65 nm thicknesses on Si substrates. For quantitative measurements of the degree of crosslinking in the polymer films, the films were immersed in chlorobenzene for 5 min, followed by rinsing with acetone, and

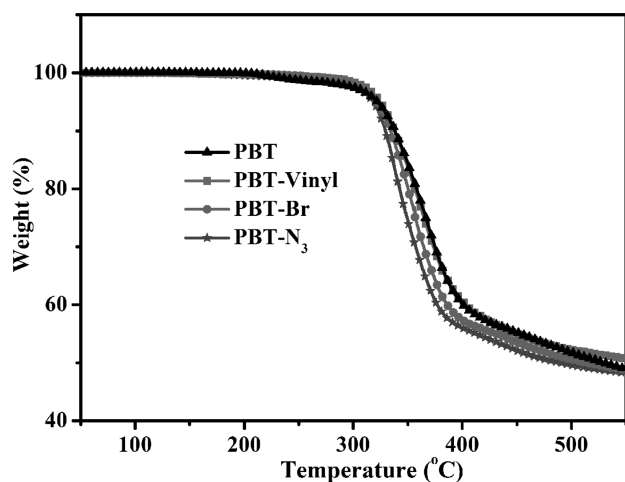


FIGURE 2 TGA thermograms of the polymers with a heating rate of $10\text{ }^{\circ}\text{C min}^{-1}$ under nitrogen.

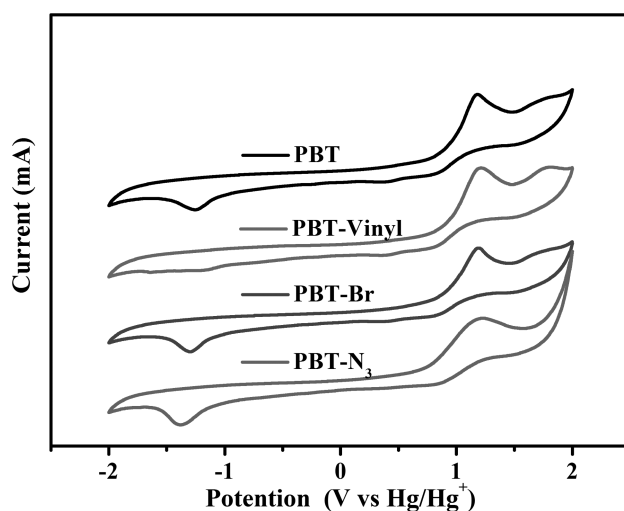


FIGURE 3 Cyclic voltammograms of PBT, PBT-vinyl, PBT-Br, and PBT- N_3 drop-cast on a Pt electrode in 0.1 mol L^{-1} Bu_4NPF_6 -acetonitrile solutions at a scan rate of 50 mV s^{-1} .

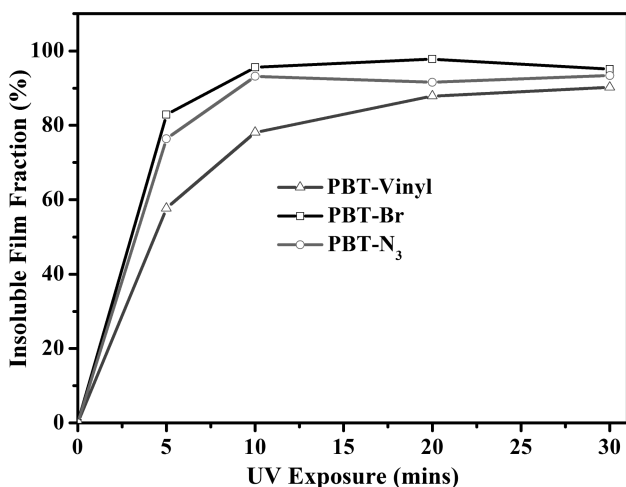


FIGURE 4 Photocrosslinking behavior of the functional PBT copolymers. The insoluble fraction was measured as a function of UV exposure time.

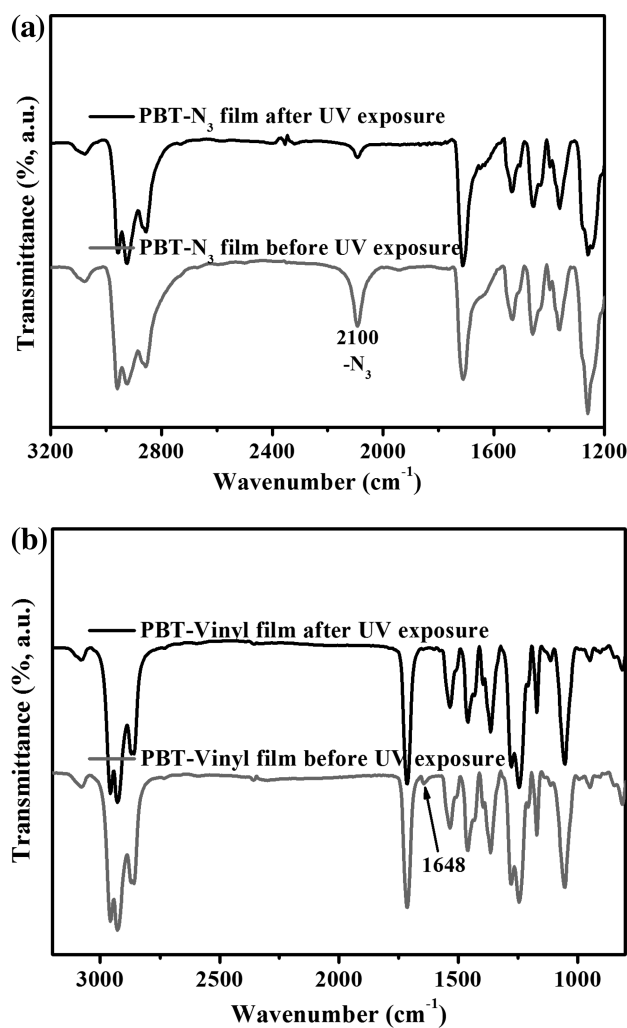


FIGURE 5 FTIR spectra of polymers (A) PBT-N₃ film and (B) PBT-vinyl film before and after UV exposure for 30 min. The characteristic IR signal for PBT-N₃ at 2100 cm⁻¹ and PBT-vinyl at 1648 cm⁻¹ were drastically decreased after UV exposure.

thicknesses of the film before and after washing were compared. For 10 min of exposure to UV light, both PBT-Br and PBT-N₃ polymers have above 90% insoluble fraction in chlorobenzene, whereas below 80% insoluble fraction was observed with the PBT-vinyl film as shown in Figure 4. After 10-min UV exposure, the PBT-Br and PBT-N₃ polymers kept almost unchangeably insoluble in chlorobenzene regardless of the UV exposure time. However, the PBT-vinyl film made a slight elevation in insoluble fraction before 30-min UV exposure. This suggests that because of different crosslinking mechanisms and reaction rates, the bromine and azide groups were presumably more prompt for photocrosslinking to yield high crosslinking density and to produce strong solvent resistance than the vinyl group.

The photocrosslinking of azide and vinyl groups were also confirmed by FTIR analysis. Figure 5 shows the FTIR spectra of PBT-N₃ and PBT-vinyl before and after UV exposure for 30 min. For the PBT-N₃, the characteristic IR signal for N₃ asymmetric stretching mode at 2100 cm⁻¹ was strongly reduced by ~95% after 30-min UV exposure, indicating the efficient photolysis of the azido groups. And for the PBT-vinyl, the

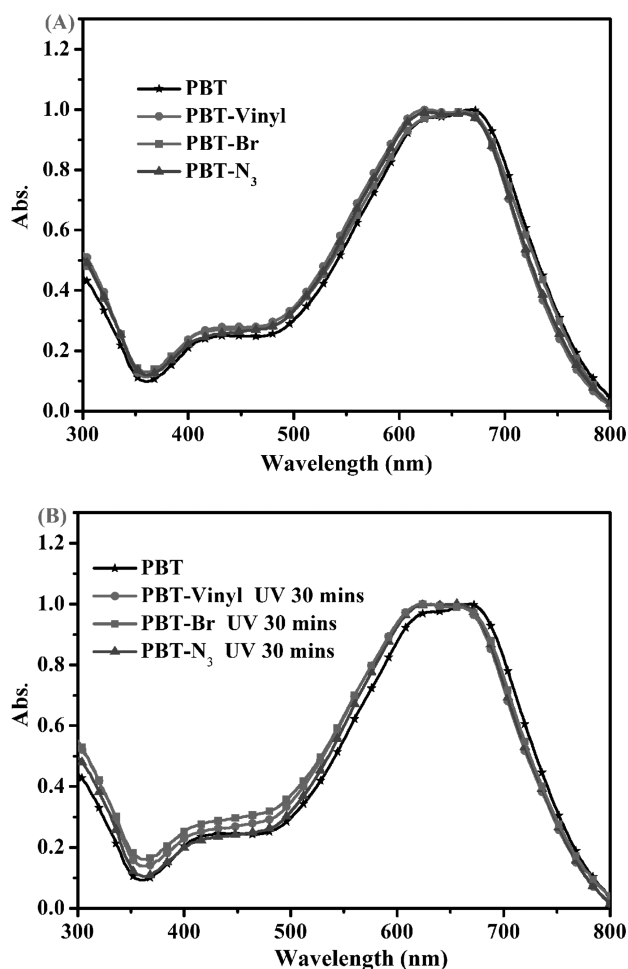


FIGURE 6 UV-vis spectra of PBT, PBT-vinyl, PBT-Br, and PBT-N₃ films (A) before and (B) after crosslinking by UV irradiation for 30 min at 254 nm.

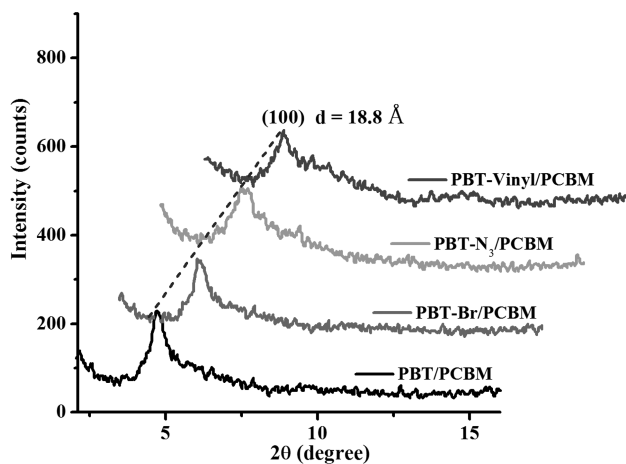


FIGURE 7 XRD patterns of the films of PBT, PBT-vinyl, PBT-Br, and PBT-N₃ blended with PCBM (copolymer:PCBM = 1:1 wt). All blend films were first exposed to UV for 30 min and then annealed for another 1 h at 150 °C.

peaks at 1648 cm⁻¹ attributed to the double bond C=C of the vinyl groups obviously disappeared in the IR spectrum after 30-min UV exposure, again undoubtedly proving the occurrence of photocrosslinking.

The normalized UV-vis absorption spectra of each polymer were acquired as thin films before and after photocrosslinking by irradiation of the films with UV light. Figure 6(a) shows both polymers exhibit the maxima between 600 and 700 nm, in accordance with previous reports.³⁹ Furthermore, no major differences in the absorption spectra can be observed between the pristine PBT and its functionalities, indicating that the addition of photocurable units to the polymer does

not significantly affect its optical properties. The absorption spectra of the polymers were essentially unchanged after 30 min of UV irradiation [Fig. 6(b)], exhibiting the same band gaps and transitions as before UV exposure, which indicates that none of the three different photocrosslinking reactions damaged the conjugated polymer backbone.

The crystallinity of copolymer in the active layer plays an important role in the hole-transport properties. XRD was employed to detect copolymers crystallinity variations in the blends containing different photocurable groups. Figure 7 shows the XRD profiles of the films of PBT, PBT-vinyl, PBT-Br, and PBT-N₃ blended with PCBM (polymers:PCBM = 1:1 wt) prepared from DCB solutions, followed by exposing to UV for 30 min and then annealed for another 1 h at 150 °C. Compared with the pure PBT blend, the crosslinked functionalized-PBT blends does not change the position of the (100) diffraction peak at $2\theta = 4.7^\circ$, corresponding to crystalline vertical stacking of the polymers chains with lamellar distance of $d = 18.8 \text{ \AA}$. Furthermore, the length scales of the copolymers crystallites at the (100) reflection in these blends can be quantified by estimating the mean size of the copolymers crystalline domain using Scherrer's equation.⁴⁰ The mean size of the pure PBT crystallite in the PBT/PCBM blend was determined to be 18.4 nm. With introducing photocrosslinkable groups into the copolymer side chain, the crystallite size only slight decreased to 18.2 nm for PBT-Br; 17.5 nm for PBT-N₃, and 17.2 nm for PBT-vinyl, respectively. The almost unchanged crystallite size means that UV crosslinking does not significantly affect the PBT crystallinity in the blend.

Deeper insight into the extreme contrast in thermal stability can be gleaned by examination of the morphology of the

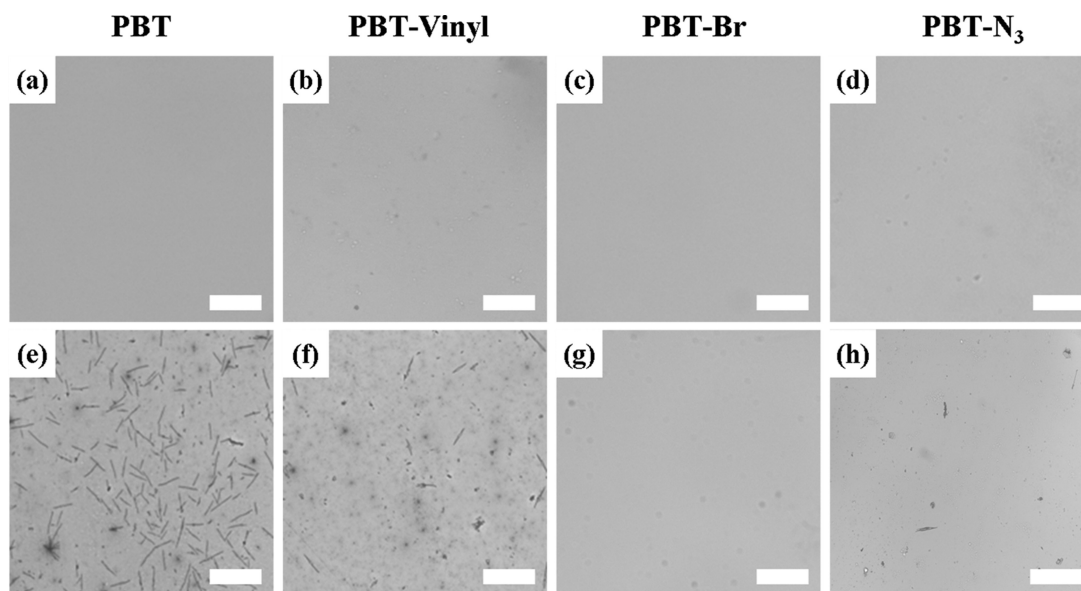


FIGURE 8 Optical microscopy images of spin-coated thin films of the four polymers blended with PCBM (1:1 wt) (a–d) before and (e–h) after annealing at 150 °C for 12 h. All the thin films have been irradiated with UV light at 254 nm for 30 min before annealing process. Scale bar = 100 μm.

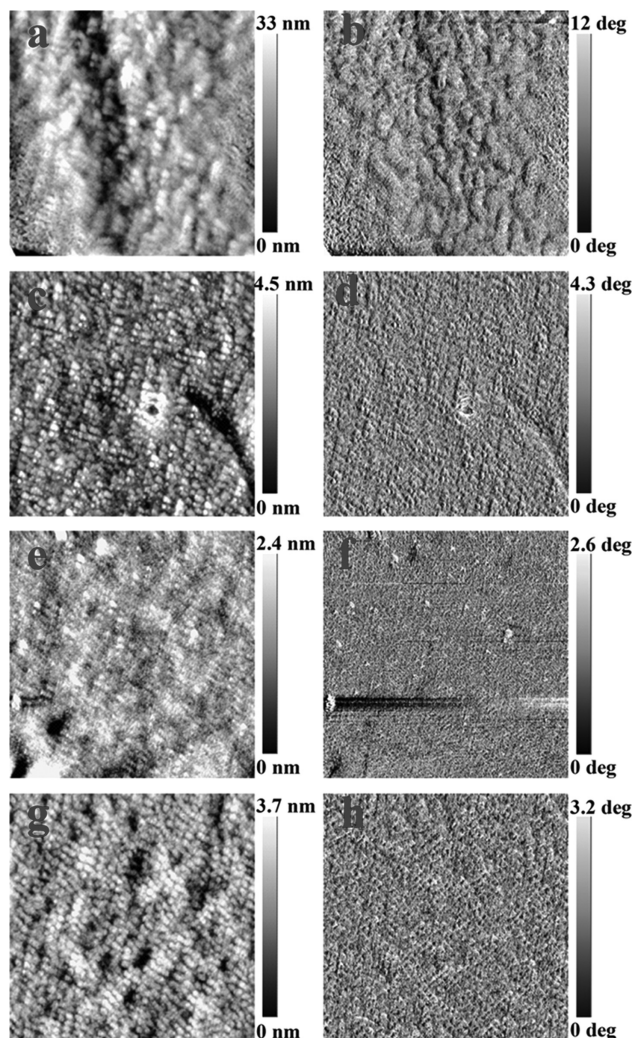


FIGURE 9 AFM topography and phase images of the (a, b) PBT, (c, d) PBT-vinyl, (e, f) PBT-Br, and (g, h) PBT-N₃ films blended with PCBM (1:1 wt). All blend films were first exposed to UV 30 min and then annealed for another 12 h at 150 °C.

active layer via optical microscopy as shown in Figure 8. As expected, thermal annealing at 150 °C for 12 h induced the formation of many needle-like PCBM crystals in the PBT/PCBM sample similar to what has been observed for annealing of P3HT/PCBM,²¹ revealing that there was severe macro-phase separation driven by the crystallization of the highly regioregular PBT polymer and PCBM molecule. In striking contrast, the blends containing PBT-Br and PBT-N₃ showed a homogeneous film with either none or only very little dark PCBM crystals, while the blend containing PBT-vinyl showed some small dark PCBM crystals but are still much smaller than those in PBT/PCBM annealed sample. This demonstrates that the photocrosslinking has taken place for all the polymers with incorporated functional groups and that the crosslinking activated by Br and N₃ groups dramatically suppresses phase segregation and stabilizes the morphology of the BHJ layer under long-term thermal annealing, thus would produce stable performance in solar cell devices.

To clarify the effect of photocrosslinking on the morphology of the active layer, AFM was also performed on both PBT and three different types of functionalized PBT films blended with PCBM (1:1 wt). After thermal annealing at 150 °C for 12 h, the non-photocrosslinked PBT active layer film [Fig. 9(a,b)] showed a very rough surface morphology with the root mean square (RMS) roughness of 25.4 nm, suggesting that a prolonged thermal annealing induced the formation of large aggregates of PCBM. This pronounced phase separation between donor and acceptor domains may yield poor contact between the active layer and the electrode, as well as unfavorable conditions for charge separation and transport. However, a significant decrease in RMS roughness was observed for the photocrosslinked PBT-vinyl film (decrease to 4.1 nm), concluding that photocrosslinking allowed locking-in the optimized active layer morphology in which the PCBM diffusion is suppressed. Obviously, the photocrosslinked PBT-Br and PBT-N₃ active layer films showed a much smoother surface, resulting in the well-developed interpenetrating network and finer nanoscale morphology. The RMS roughness further decrease to 1.7 nm for PBT-Br and 2.3 nm for PBT-N₃-annealed blend films, ascribing to the denser crosslinking network maintaining the homogenous morphology.

To obtain more information of the effect of photocrosslinking on the polymer/PCBM two-phased structure, its morphology was further investigated by TEM. TEM samples of the BHJ layers were prepared by first employing UV-mediated photocrosslinking for 30 min and then annealed for another 12 h at 150 °C. The planar TEM images presented in Figure 10 for samples are similar to the results observed in the AFM and

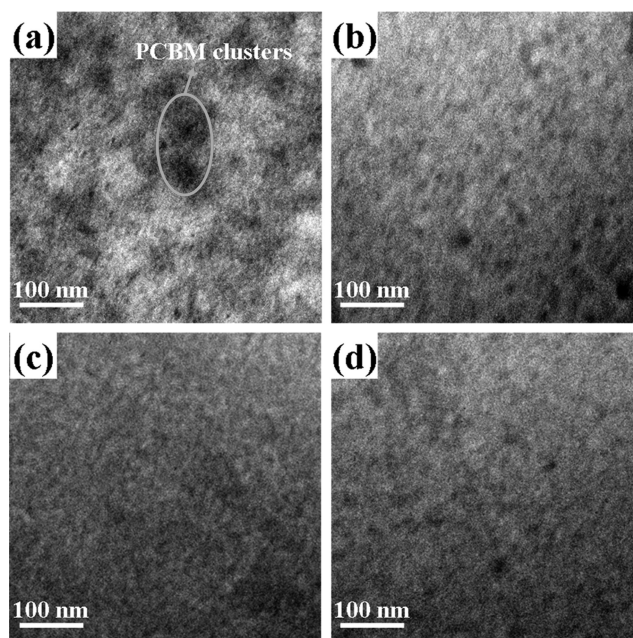


FIGURE 10 TEM images of the (a) PBT, (b) PBT-vinyl, (c) PBT-Br, and (d) PBT-N₃ films blended with PCBM (1:1 wt). All blend films were first exposed to UV 30 min and then annealed for another 12 h at 150 °C.

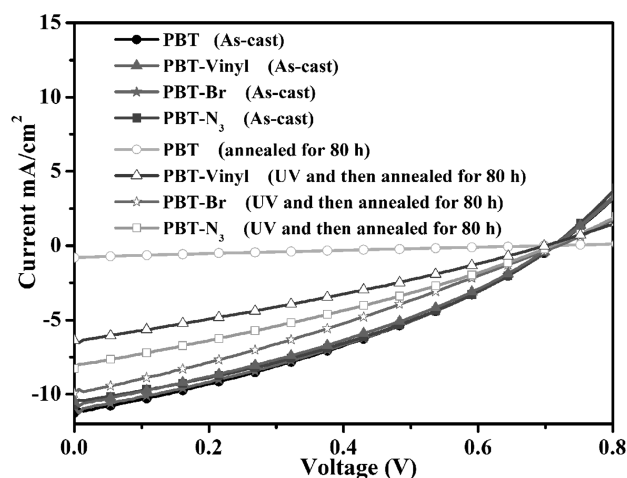


FIGURE 11 J - V characteristics of the photocrosslinked PBT-vinyl/PCBM, PBT-Br/PCBM, and PBT- N_3 /PCBM blends compared with the nonphotocrosslinked PBT/PCBM blend before and after annealing at 150 °C for 80 h.

optical microscopy images. They can be distinguished from the dark area and bright area as they have clear boundaries, where the bright and dark parts represent the polymer-rich and PCBM-rich domains, respectively. After thermal annealing at 150 °C for 12 h, the PBT sample showed a coarse morphology with larger dark and bright as reflecting extended phase separation in Figure 10(a), whereas the photocrosslinked PBT-vinyl sample presented dramatically decreased size of the phase-separated domains in spite of the existence of some smaller PCBM domains in Figure 10(b). For the PBT-Br and PBT- N_3 samples, the photocrosslinking films were characterized by a slight variation reflecting a rather well-distributed and finer phase-separated structure compared to the photocrosslinked PBT-vinyl film. Especially for the PBT-Br sample, the TEM image showed the most homogeneous domain of equal size with the fine intermixing between PBT and PCBM. From these results, we confirm that photocrosslinking allows stabilizing the morphology of the active layer and prevents the aggregation of PCBM even after long-term annealing, and Br and N_3 photocurable groups promote the tendency.

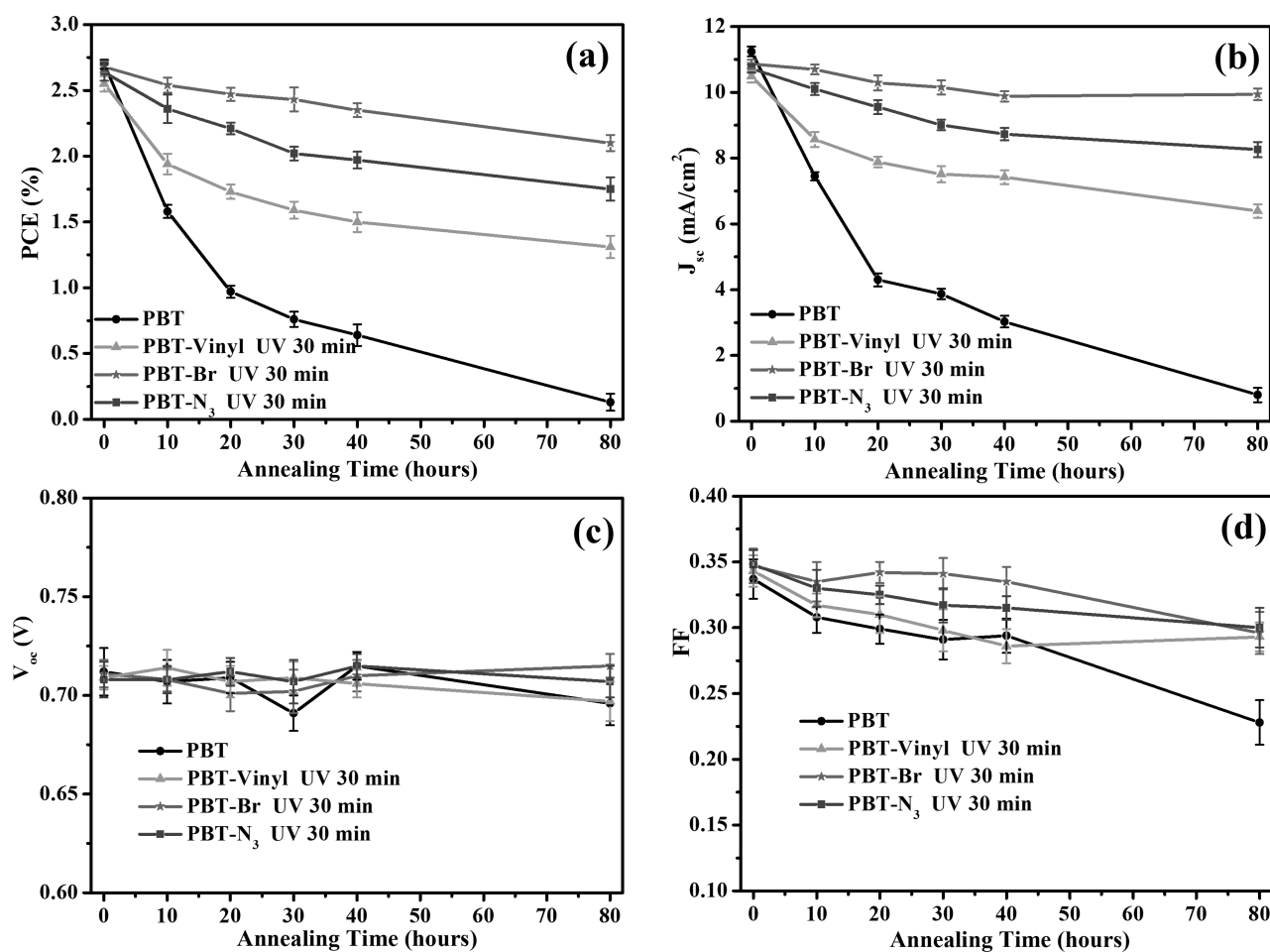


FIGURE 12 Photovoltaic characteristics of the photocrosslinked PBT-vinyl/PCBM, PBT-Br/PCBM, and PBT- N_3 /PCBM blends compared with the nonphotocrosslinked PBT/PCBM blend with varying vacuum annealing duration at 150 °C up to 80 h. (a) PCE, (b) J_{sc} , (c) V_{oc} , and (d) FF. Data points represent average values of three measured devices, with error bars denoting one standard deviation.

TABLE 2 Solar Cell Performance Parameters of PBT/PCBM, PBT-vinyl/PCBM, PBT-Br/PC₆₁BM, and PBT-N₃/PC₆₁BM (1:1 wt) Blends

Components	Thickness (nm)	V _{oc} (V)	J _{sc} (mA cm ⁻²)	FF	PCE ^a (%)
PBT:PCBM ^b	80	0.712	11.24	0.337	2.70
PBT:PCBM ^c	80	0.696	0.80	0.228	0.13
PBT-vinyl:PCBM ^b	80	0.708	10.48	0.343	2.55
PBT-vinyl:PCBM ^d	80	0.697	6.39	0.293	1.31
PBT-Br:PCBM ^b	80	0.711	10.86	0.347	2.68
PBT-Br:PCBM ^d	80	0.714	9.94	0.296	2.10
PBT-N ₃ :PCBM ^b	80	0.708	10.72	0.348	2.64
PBT-N ₃ :PCBM ^d	80	0.707	8.26	0.300	1.75

^a All values represent averages.

^b As-cast blend film.

^c Annealing for 80 h at 150 °C.

^d Active layers were first exposed to UV for 30 min and then annealed for another 80 h at 150 °C.

To investigate the effect of crosslinking on the performance and thermal stability, we subjected optimized UV-crosslinked PBT-vinyl (exposed to UV for 30 min), PBT-Br and PBT-N₃ blended with PCBM solar cells to 150 °C (in vacuum) for as long as 80 h and compare device performance with uncrosslinked PBT/PCBM blend-based device. The devices with the configuration of ITO/PEDOT:PSS/polymer:PCBM/LiF/Al were prepared for each of the four polymers. Figure 11 and Table 2 show the performances of these devices before and after thermal annealing at 150 °C for 80 h. Before annealing, it is noteworthy that all four devices exhibit similar efficiency of ~2.6 %, which is close to the results of polymers with a similar structure reported in the literature.^{41,42} This indicates that the incorporation of photocurable substituents at the end of the alkyl chain of PBT does not affect solar cell performance under UV exposure. However, they showed a dramatic contrast in thermal stability after annealing at an elevated temperature of 150 °C, which serves as an accelerated performance test. The device performance of the pristine-PBT/PCBM blend decreased rapidly to less than 10% of its initial efficiency value after 80 h annealing at 150 °C, as seen in Figure 12. On the contrary, the performance of both PBT-Br and PBT-N₃ devices with UV irradiation for 30 min, followed by 80 h annealing at 150 °C, showed very stable device performance with 78 and 66% initial device efficiency, respectively. Interestingly, the performance of solar cell based on photocrosslinkable PBT-vinyl retained only 51% of its initial value under long-time thermal annealing. The difference of behavior between the three functionalized polymers solar cells indicates that the density crosslinking network induced by different photocurable groups greatly influences the device stability, and a proper crosslinking degree with homogenous active morphology could dramatically enhance the device stability, but without sacrificing the performance.

The nonphotocrosslinked PBT/PCBM devices underwent a sharp decrease in PCE primarily due to the significant decrease in short-circuit current density (J_{sc}) and the slight reduction in fill factor (FF) after annealing as shown in Figure 12. The decrease in J_{sc} and FF stems from an increased device serial resistance was caused by the large phase separation morphology after annealing,²⁹ as observed by the AFM and TEM images. Conversely, the open-circuit voltage (V_{oc}) of all devices remained constant, even after 80 h of annealing at 150 °C, which indicates that the V_{oc} in BHJ solar cells is linearly dependent on the magnitude of the built-in potential, defined as the difference between the HOMO level of a p-type donor and the LUMO level of an n-type acceptor,⁴³ rather than the change in blend phase separation morphology. This demonstrates that photocrosslinking has allowed an optimal morphology of the active layer to mostly be preserved throughout the entire annealing process, thus leading to remarkable long-term thermal stability of these devices.

CONCLUSIONS

We have presented a comparative study between three different types of photocrosslinkable low band-gap donor-acceptor-conjugated polymers. Three functional copolymers were prepared by introducing vinyl, bromine, and azide photocurable groups into the side chains of PBT copolymer with relatively simple means. Incorporation of these groups does not change the thermal stability and disrupt the overall crystallinity and optical property of the copolymers when compared to the pristine PBT copolymer. The crosslinking reaction could be easily achieved by UV-irradiation of the functional copolymers to give solvent-resistant films. Presumably, because of different crosslinking mechanisms and reaction rates, the bromine and azide groups were more prompt for photocrosslinking to yield high crosslinking density and to produce strong solvent resistance than the vinyl group. In addition, these functional copolymers are used in BHJ solar cells with PCBM to investigate the effect of photocurable groups on the device performance and stability. After thermal annealing at 150 °C for 80 h, the crosslinked PBT-Br and PBT-N₃ copolymers showed very thermally stable photovoltaic device performance by retaining 78 and 66% of their initial device efficiency, respectively, whereas PBT-vinyl devices retained only 51% of its initial value. The difference in device stability between these functional copolymers solar cells should be ascribed to different crosslinking density presumably resulting from different reaction rates and crosslinking mechanisms of these photocurable groups. However, the same devices with pristine-PBT/PCBM devices decreased rapidly to less than 10% of its initial efficiency value. This demonstrates that photocrosslinking can improve the thermal stability of the active layer by suppressing PCBM diffusion and phase separation, and thus leading to thermally stable device performance.

ACKNOWLEDGMENTS

This work was supported by the National Natural Science Foundation of China (51263016 and 51003045).

REFERENCES AND NOTES

- 1 C. J. Brabec, N. S. Sariciftci, J. C. Hummelen, *Adv. Funct. Mater.* **2001**, *11*, 15–26.
- 2 S. H. Park, A. Roy, S. Beaupre, S. Cho, N. Coates, J. S. Moon, D. Moses, M. Leclerc, K. Lee, A. J. Heeger, *Nat. Photon.* **2009**, *3*, 297–303.
- 3 G. Yu, J. Gao, J. C. Hummelen, F. Wudl, A. J. Heeger, *Science* **1995**, *270*, 1789–1791.
- 4 H. Chen, J. Hou, S. Zhang, Y. Liang, G. Yang, Y. Yang, L. Yu, Y. Wu, G. Li, *Nat. Photon.* **2009**, *3*, 649–653.
- 5 R. F. Service, *Science* **2011**, *332*, 293–293.
- 6 S. E. Shaheen, C. J. Brabec, N. S. Sariciftci, F. Padinger, T. Fromerz, J. C. Hummelen, *Appl. Phys. Lett.* **2001**, *78*, 841–843.
- 7 G. Li, V. Shrotriya, J. S. Huang, Y. Yao, T. Moriarty, K. Emery, Y. Yang, *Nat. Mater.* **2005**, *4*, 864–868.
- 8 A. Pivrikas, P. Stadler, H. Neugebauer, N. S. Sariciftci, *Org. Electron.* **2008**, *9*, 775–782.
- 9 J. Peet, J. Y. Kim, N. E. Coates, W. L. Ma, D. Moses, A. J. Heeger, G. C. Bazan, *Nat. Mater.* **2007**, *6*, 497–500.
- 10 J. Jo, S. I. Na, S. S. Kim, T. W. Lee, Y. Chung, S. J. Kang, D. Vak, D. Y. Kim, *Adv. Funct. Mater.* **2009**, *19*, 2398–2406.
- 11 S. S. Van Bavel, E. Sourty, G. De With, J. Loos, *Nano Lett.* **2009**, *9*, 507–513.
- 12 B. Paci, A. Generosi, V. Rossi Albertini, R. Generosi, P. Perfetti, R. De Bettignies, C. Sentein, *J. Phys. Chem. C* **2008**, *112*, 9931–9936.
- 13 G. Li, V. Shrotriya, Y. Yao, Y. Yang, *J. Appl. Phys.* **2005**, *98*, 043704.
- 14 M. Helgesen, M. Bjerring, N. C. Nielsen, F. C. Krebs, *Chem. Mater.* **2010**, *22*, 5617–5624.
- 15 J. Zhao, A. Swinnen, G. Van Assche, J. Manca, D. Vanderzande, B. Van Mele, *J. Phys. Chem. B* **2009**, *113*, 1587–1591.
- 16 S. Bertho, G. Janssen, T. M. Cleij, B. Conings, W. Moons, A. Gadisa, J. D. Goovaerts, L. Lutsen, J. Manca, D. Vanderzande, *Sol. Energy Mater. Sol. Cells* **2008**, *92*, 753–760.
- 17 J. Vandenberg, B. Conings, S. Bertho, J. Kesters, D. Spoltore, S. Esiner, J. Zhao, G. Van Assche, M. M. Wienk, W. Maes, L. Lutsen, B. Van Mele, R. A. J. Janssen, J. Manca, D. J. M. Vanderzande, *Macromolecules* **2011**, *44*, 8470–8478.
- 18 K. Sivula, Z. T. Ball, N. Watanabe, J. M. J. Frechet, *Adv. Mater.* **2006**, *18*, 206–210.
- 19 M. Drees, H. Hoppe, C. Winder, H. Neugebauer, N. S. Sariciftci, W. Schwinger, F. Schaffler, C. Topf, M. C. Scharber, Z. G. Zhu, R. Gaudiana, *J. Mater. Chem.* **2005**, *15*, 5158–5163.
- 20 Z. Zhu, S. Hadjikyriacou, D. Waller, R. Gaudiana, *Macromol. J. Sci. Part A: Pure Appl. Chem.* **2004**, *41*, 1467–1487.
- 21 B. J. Kim, Y. Miyamoto, B. W. Ma, J. M. J. Frechet, *Adv. Funct. Mater.* **2009**, *19*, 2273–2281.
- 22 J. M. J. Frechet, G. Griffini, J. D. Douglas, C. Piliago, T. W. Holcombe, S. Turri, J. L. Mynar, *Adv. Mater.* **2011**, *23*, 1660–1664.
- 23 A. Charas, Q. Ferreira, J. Farinhas, M. Matos, L. Alcacer, J. Morgado, *Macromolecules* **2009**, *42*, 7903–7912.
- 24 I. R. Gearba, C. Y. Nam, R. Pindak, C. T. Black, *Appl. Phys. Lett.* **2009**, *95*, 173307.
- 25 A. E. A. Contoret, F. Sr, M. O'Neill, J. E. Nicholls, G. J. Richards, S. M. Kelly, A. W. Hall, *Chem. Mater.* **2002**, *14*, 1477–1487.
- 26 Y. F. Li, Y. P. Zou, *Adv. Mater.* **2008**, *20*, 2952–2958.
- 27 B. Gholamkhash, S. Holdcroft, *Chem. Mater.* **2010**, *22*, 5371–5376.
- 28 H. J. Kim, A. R. Han, C. H. Cho, H. Kang, H. H. Cho, M. Y. Lee, J. M. J. Frechet, J. H. Oh, B. J. Kim, *Chem. Mater.* **2012**, *24*, 215–221.
- 29 C. Y. Nam, Y. Qin, Y. S. Park, H. Hlaing, X. Lu, B. M. Ocko, C. T. Black, R. B. Grubbs, *Macromolecules* **2012**, *45*, 2338–2347.
- 30 C. H. Hsieh, Y. J. Cheng, P. J. Li, C. H. Chen, M. Dubosc, R. M. Liang, C. S. Hsu, *J. Am. Chem. Soc.* **2010**, *132*, 4887–4893.
- 31 U. R. Lee, T. W. Lee, M. H. Hoang, N. S. Kang, J. W. Yu, K. H. Kim, K. G. Lim, T. W. Lee, J. I. Jin, D. H. Choi, *Org. Electron.* **2011**, *12*, 269–278.
- 32 Y. Yao, Y. Y. Liang, V. Shrotriya, S. Q. Xiao, L. P. Yu, Y. Yang, *Adv. Mater.* **2007**, *19*, 3979–3983.
- 33 R. Q. Png, P. J. Chia, J. C. Tang, B. Liu, S. Sivaramakrishnan, M. Zhou, S. H. Khong, H. S. O. Chan, J. H. Burroughes, L. L. Chua, R. H. Friend, P. K. H. Ho, *Nat. Mater.* **2010**, *9*, 152–158.
- 34 J. H. Hou, Z. A. Tan, Y. Yan, Y. J. He, C. H. Yang, Y. F. Li, *J. Am. Chem. Soc.* **2006**, *128*, 4911–4916.
- 35 K. S. Lee, K. Y. Yeon, K. H. Jung, S. K. Kim, *J. Phys. Chem. A* **2008**, *112*, 9312–9317.
- 36 R. F. Klima, A. D. Gudmundsdottir, *J. Photochem. Photobiol. A* **2004**, *162*, 239–247.
- 37 K. A. Murray, A. B. Holmes, S. C. Moratti, G. Rumbles, *J. Mater. Chem.* **1999**, *9*, 2109–2116.
- 38 J. Lowe, S. Holdcroft, *Macromolecules* **1995**, *28*, 4608–4616.
- 39 Y. Y. Liang, Y. Wu, D. Q. Feng, S. T. Tsai, H. J. Son, G. Li, L. P. Yu, *J. Am. Chem. Soc.* **2009**, *131*, 56–57.
- 40 B. D. Cullity, S. R. Stock, *Elements of X-ray Diffraction*, 3rd ed.; Prentice Hall: New York, **2001**, pp 167–171.
- 41 S. Wakim, S. Alem, Z. Li, Y. Zhang, S.-C. Tse, J. P. Lu, J. F. Ding, Tao. Y. *J. Mater. Chem.* **2011**, *21*, 10920–10928.
- 42 J. H. Huang, X. Wang, C. L. Zhan, Y. Zhao, Y. X. Sun, Q. B. Pei, Y. Q. Liu, J. N. Yao, *Polym. Chem.* **2013**, *4*, 2174–2182.
- 43 M. Lenes, G.-J. A. H. Wetzelaer, F. B. Kooistra, S. C. Veenstra, J. C. Hummelen, P. W. M. Blom, *Adv. Mater.* **2008**, *20*, 2116–2119.